Research on the Preparation of Zirconia Coating on Titanium Alloy Surface and Its Tribological Properties

Qiancheng Zhao [1], Li Wang [2], Tianchang Hu [1,*], Junjie Song [1,*], Yunfeng Su [1] and Litian Hu [1]

1 Lanzhou Institute of Chemical Physics, Chinese Academic of Sciences, Lanzhou 730000, China; acefieyanjuny@outlook.com (Q.Z.); yfsu@licp.cas.cn (Y.S.); lthu@licp.cas.cn (L.H.)

2 Hangzhou Xiolift Company Limited, Hangzhou 311103, China; wangli_2@xiolift.com

* Correspondence: htchang@licp.cas.cn (T.H.); songjunjie@licp.cas.cn (J.S.)

Abstract: Titanium alloys have been widely used in aerospace and other fields due to their excellent properties such as light weight and high strength. However, the extremely poor tribological properties of titanium alloys limit their applications in certain special working conditions. In order to improve the tribological properties of titanium alloys, the zirconia coatings were prepared on the surface of a TC4 titanium alloy using the discharge plasma sintering method in this article. The influence of sintering parameters on properties such as density, adhesion, hardness, and phase composition, as well as tribological properties (friction coefficient, wear rate) were investigated, and the influence mechanism of the coating structure on its mechanical and frictional properties was analyzed. The results showed that, with the increase in sintering temperature, the density, bonding strength, and hardness of the zirconia coating were significantly improved. The zirconia coating prepared at a sintering temperature of 1500 °C and a sintering time of 20 min had the lowest friction coefficient and wear rate, which are 0.33 and 6.2×10^{-8} cm$^3 \cdot$N$^{-1} \cdot$m^{-1}, respectively. Numerical analysis showed that the increase in temperature and the extension of time contributed to the extension of the diffusion distance between zirconia and titanium, thereby improving the interfacial adhesion. The influence mechanism of different sintering temperatures and sintering times on the wear performance of zirconia coatings was explained through Hertz contact theory.

Keywords: TC4 titanium alloy; zirconia; spark plasma sintering; wear resistant coating

1. Introduction

Titanium alloys are a widely used light metal material with advantages, such as high strength, good corrosion resistance, strong heat resistance, and lower density than steel, which has attracted widespread attention from scientists. At present, they have been widely used in various fields such as aviation, biomedicine, and shipbuilding [1]. However, titanium alloys have low hardness, a high friction coefficient, and poor wear resistance, especially when used as friction pairs, which often leads to material damage and reduces their service life, limiting their applications [2]. Currently, in order to improve the tribological properties of titanium alloys, scholars have performed a lot of work, among which a large amount of research, which has been required to improve the friction properties of titanium alloys through surface coating or surface modification methods, including shot peening [3], micro-arc oxidation [4], thermal spraying [5], laser cladding [6], PVD [7], CVD [8], nitriding [9], and laser texturing [10], etc. The research on the application of anti-wear coatings will be the main direction of future research. The commonly used materials for wear-resistant coatings include metals [11], ceramics [12], composite materials [13], and other types. Metal material coatings have good conductivity and thermal conductivity, high toughness, and good ductility, making them easy to coat on the surface of materials and undergo some chemical modifications [14]. Ceramic material coatings have the advantages of a high melting point, high hardness, good wear resistance, and strong corrosion

resistance. Compared to metal coatings, there is less research on the friction performance of ceramic coatings on titanium alloy surfaces.

Generally, ceramic coatings such as alumina [15], silicon carbide [16], and zirconia [17] are prepared by vapor deposition or thermal spraying. Zirconia, as an important high-temperature resistant ceramic material with a high melting point and low coefficient of thermal expansion, is often used in fields such as thermal barrier coatings, artificial teeth, refractory materials [18]. The hardness of ZrO_2 is much higher than that of a titanium alloy, so it is expected to be used as a wear-resistant coating material for titanium alloys. However, ceramic coatings have problems, such as weak adhesion to metal substrates and susceptibility to brittle cracking. At the same time, ceramic coatings also have low compactness and require post-treatment. Therefore, how to achieve effective bonding of ceramic coatings on titanium alloy substrates and improve coating density provides a research basis for improving the tribological properties of titanium alloy materials under harsh working conditions. This is also of great significance for further expanding the tribological applications of titanium alloys.

Spark plasma sintering (SPS) is a type of ultra-fast densification sintering of materials using heating and surface activation. It has the advantages of a fast heating rate, short sintering time, low sintering temperature, uniform heating, high production efficiency, and energy conservation. In addition, due to the combined effect of plasma activation and rapid heating sintering, the growth of grains is suppressed and the microstructure of the original particles is maintained. The performance of the sintered body is fundamentally improved. The final product has the characteristics of a small and uniform structure, maintaining the natural state of the raw material with high density. Compared with hot pressing sintering and hot isostatic pressing sintering, the SPS device is simpler to operate, and this technology can be applied not only to the preparation of ceramic materials [19], but also to the preparation of a metal matrix and ceramic composite connecting materials [20].

Therefore, we plan to use discharge plasma sintering to prepare zirconia coatings on the surfaces of titanium alloys in order to improve the tribological performance of titanium alloys under different working conditions. The influence of different sintering parameters on the mechanical properties of zirconia coatings was revealed, and the wear mechanism and suitable preparation process of zirconia coatings under different operating conditions were proposed.

2. Materials and Methods

In the experiment, the TC4 titanium alloy (Ti-6Al-4V, ø24 mm × 7.9 mm, Baoji Licheng titanium metal material Co., Ltd., Baoji, China) was selected as the substrate. Then, the surfaces were ground sequentially with 180#, 800#, and 2000# silicon carbide sandpapers. Next, the samples were polished by using the grinding paste, and finally, the samples were ultrasonically cleaned in ethanol and dried before use.

The mass fraction of tetragonal phase (PDF:50-1089) in zirconia powder (JiangSu Lida high-tech special Materials Co., Ltd., Changshu, China) is 69.2%, and the mass fraction of Baddeleyite (PDF:37-1484) is 30.8%. The preparation process of the coating is shown in Figure 1. A total of 0.57 g of zirconia powder was added to a certain amount of ethanol and stirred evenly. The 0.2 mm thick square graphite paper was attached to the inner wall of the SPS mold, and then a pressure rod and gasket were placed at the bottom. After this, a 0.3 mm thick graphite paper was placed on the surface of the gasket, and then the polished TC4 titanium alloy block was placed on top. The previously prepared zirconia suspension was poured into the mold and left to stand for 2 h. A uniform coating of zirconia was formed on the surface of TC4 after the ethanol evaporating, and then the SPS mold was installed in the discharge plasma sintering furnace (RP-S type, Shanghai Chenhua Technology Co., Ltd., Shanghai, China) for sintering. By adjusting the different sintering process parameters such as heating temperature, heating time, and sintering time, a series of coatings were prepared.
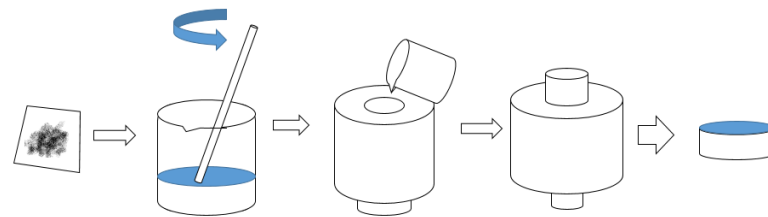
Figure 1. Preparation process diagram of zirconia coating.

After cooling, residual graphite paper was removed from the coating surface by using a 180 # silicon carbide sandpaper. Figure 1 and Table 1, respectively, present the schematic diagrams of the sintering process and sintering parameters used in this experiment. The method of vacuum sintering without pressure was used in the experiment.

Table 1. SPS sintering process parameters.

Process Name	Temperature Rising Time (min)	Sintering Temperature (°C)	Sintering Time (min)
950	10	950	3
1000	7	1000	2
1050	11	1050	2
1200	16	1200	15
1250	13	1250	15
1300	16	1300	15
1400	16	1400	15
1000 A	11	1000	15

Tribological tests were performed using the reciprocating friction and wear machine (GF-1200 model, Lanzhou Zhongke Kaihua Technology Development Co., Ltd., Lanzhou, China) for testing. A schematic diagram of the testing device is shown in Figure 2. The Si_3N_4 ceramic ball with a diameter of 6 mm was selected as the upper sample. The experimental parameters are set as follows: reciprocating length of 5 mm, loads of 10–60 N, frequency of 3.33 Hz, and a running time of 30 min.
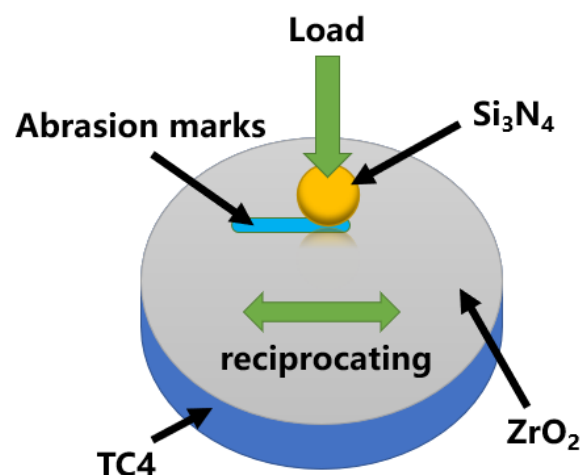

Figure 2. Schematic diagram of reciprocating friction and wear.

The surface morphologies and the wear volumes of wear tracks were measured using a 3D profilometer (VHX-6000, Keyence Company, Osaka, Japan). The formula for calculating the wear rate W is as follows:

$$W = \frac{\Delta V}{Pd} \tag{1}$$

In this formula, ΔV is the wear volume and d is sliding distance. The testing load is symbolized by P. The hardness of the coating is tested using a Vickers hardness tester with an indenter of 0.2 kg.

The adhesion strength of the coating is measured using a multifunctional material surface scratch tester (MFT-4000, Lanzhou Huahui Instrument Technology Co., Ltd., Lanzhou, China). The density of ZrO_2 coating is measured by wearing a certain thickness through sandpaper, and calculating the mass and volume of the loss part. The diameter, height, and mass of the sample are measured by vernier caliper and analytical balance.

The phase analysis of coatings is performed using an X-ray diffractometer (XRD, Empyrean, malvern panalytical, Malvern, England) with a scanning angle of 5–100°, 0.1 degrees per step, and 0.6 s per step. (Target material: Cu target, Kα = 1.54 angstroms, current = 20 mA, scanning speed 0.2°/s). The surface micro-morphologies of the coatings are characterized using scanning electron microscopy (SEM, JSM-5600LV, Japan Electronics Co., Ltd., Tokyo, Japan), combined with EDS spectroscopy to analyze the distribution of elements. The pressing depth and the stress distribution around the contact point are simulated by Hertzian contact theory.

3. Results and Discussion

3.1. The Analysis of Physical Properties of Zirconia Coatings

Figure 3 shows the morphology of zirconia coatings prepared by sintering on the surface of titanium alloy. It can be seen that the zirconia coating prepared by plasma sintering can uniformly cover the surface of the titanium alloy, and the coating is usually white after post-treatment with grinding. Microscopic observation of the surface of the coating reveals that it is relatively dense and free from defects such as cracks.
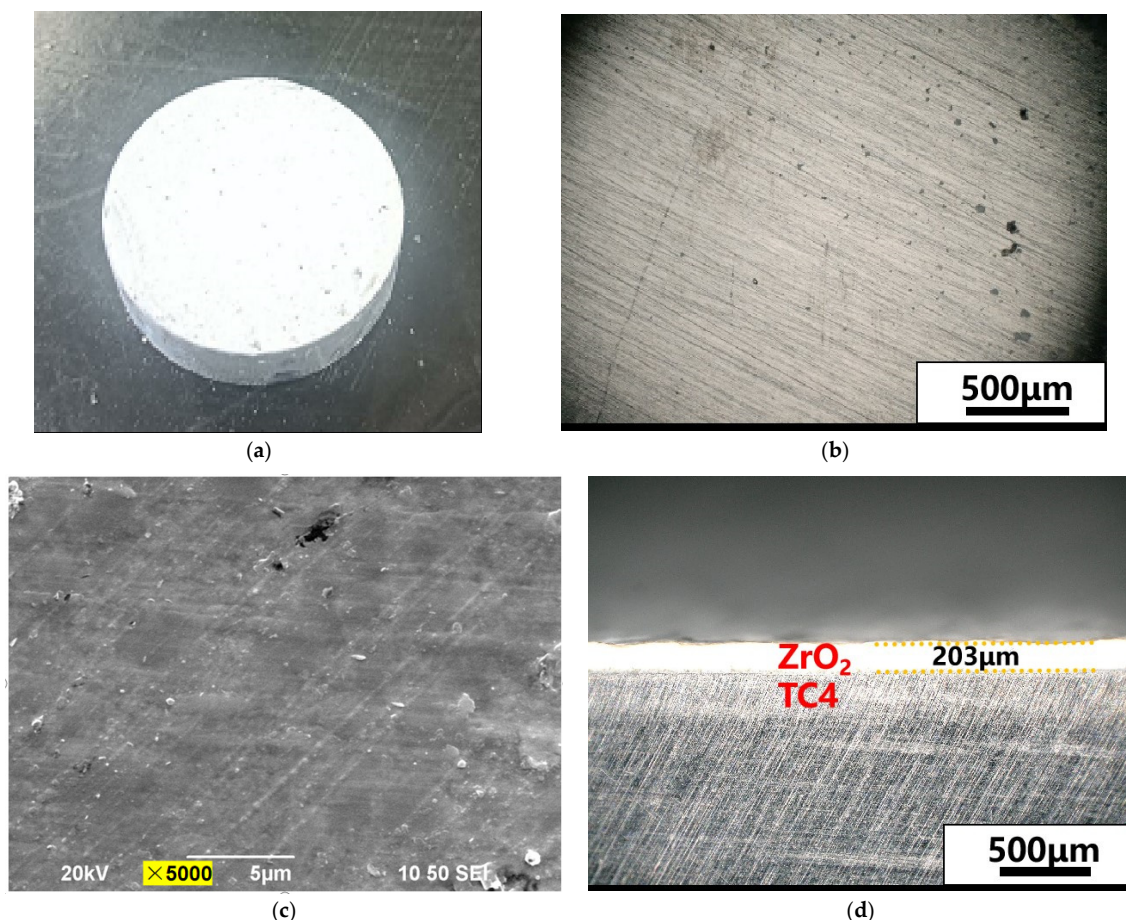

Figure 3. Morphology of zirconia coating on titanium alloy surface: (**a**) camera (**b**) optical microscopy (**c**) scanning electronic microscope (**d**) cross section.

The densities of zirconia coatings at different sintering temperatures were measured. From Table 2, it can be seen that the density of the coating gradually increases with the increase in sintering temperature and time. This may be related to the decrease in porosity caused by the surface energy of grain boundaries driving grain growth during the sintering process.

Table 2. The density of the Zirconia coatings.

Coating Sample	Density (g/cm^3)
ZrO_2-1000	4.72
ZrO_2-1200	5.37
ZrO_2-1400	5.64

Figure 4 shows a comparison of hardness between TC4 and zirconia coatings prepared at different temperatures. With the increase in sintering temperature, the hardness of the zirconia coatings has a significant difference. Zirconia coatings prepared by sintering above 1200 °C often have high hardness, while coatings generally show lower hardness when below this sintering temperature. This is mainly due to the phase transition of zirconia at higher temperatures. In addition, the coatings sintered at higher temperatures are denser, which also affects the hardness of the zirconia coating.
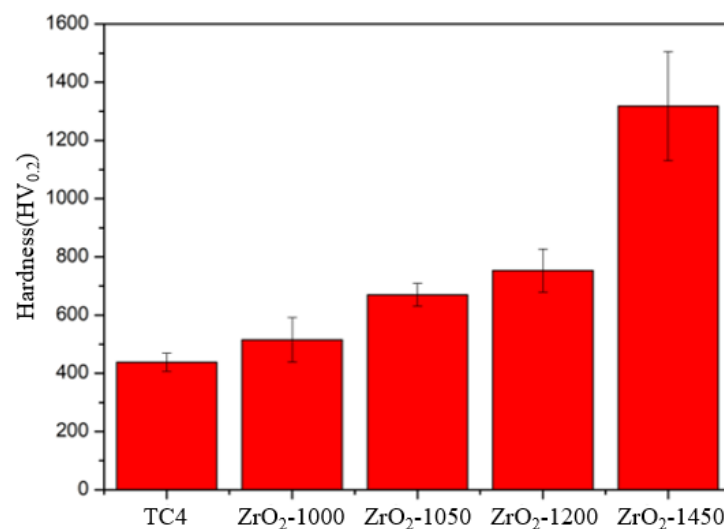

Figure 4. Hardness of TC4 and ZrO_2 coatings prepared at different temperatures.

At the same time, phase analysis was performed on the zirconia coatings, as shown in Figure 5. It is found that the ZrO_2 coating prepared at different temperatures has different phases: the monoclinic phase and the tetragonal phase. With the increases in sintering temperature, the phase of the coating changes from only the ZrO_2 monoclinic phase to a coexistence of the two phases, with a decrease in the monoclinic phase, and finally a complete transformation into a tetragonal phase. An increase in sintering temperature is beneficial for transforming the monoclinic phase into a tetragonal phase. Comparing the ZrO_2-1000 and ZrO_2-1000A coatings, it can be seen that at the same sintering temperature of 1000 °C, prolonging the sintering time is beneficial for the transformation from the monoclinic phase to the tetragonal phase. The tetragonal ZrO_2 has a higher hardness, and can undergo a longer sintering time and a higher sintering temperature. Therefore, to prepare the coatings with good mechanical properties, it is necessary to use sintering temperatures above 1200 °C and longer sintering times during the preparation process.
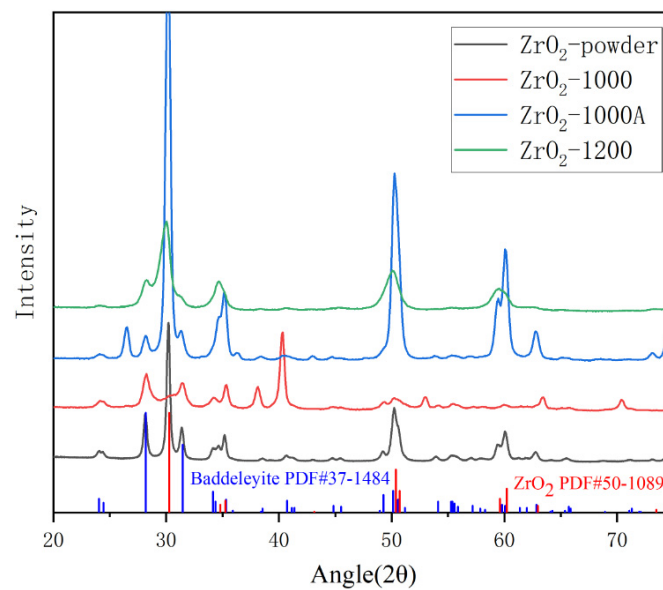
Figure 5. XRD analysis of zirconia coatings prepared under different conditions.

Based on the above experimental results, sintering temperatures above 1300 °C were selected for the preparation of zirconia coatings, and the effects of different sintering temperatures and times on their friction properties were investigated. The preparation process of the coating is the same as in Section 2. Table 3 provides the sintering parameters in this experiment.

Table 3. Sintering process parameters.

Process Name	Temperature Rising Time (min)	Sintering Temperature (°C)	Sintering Time (min)
1300A10	16	1300	10
1300A15	16	1300	15
1300A20	16	1300	20
1300A25	16	1300	25
1400A10	16	1400	10
1400A15	16	1400	15
1400A20	16	1400	20
1400A25	16	1400	25
1500A10	16	1500	10
1500A15	16	1500	15
1500A20	16	1500	20
1500A25	16	1500	25

Figure 6 shows the trend of the bonding force between the zirconia coating and the titanium alloy substrate as a function of the sintering temperature and sintering time. It can be seen that, at the sintering temperature of 1300 °C with the prolongation of the sintering time, the bonding force between the coating and the substrate gradually increases from 34 N to around 55 N. Similar trends are also observed at other sintering temperatures. When the sintering time is selected as 25 min, the increase in the sintering temperature results in a small change in the coating bonding force, which is basically maintained at around 53 N. When the sintering temperature is between 1300–1500 °C, the influence of temperature on the bonding force is relatively small and the main influencing factor is the sintering time.
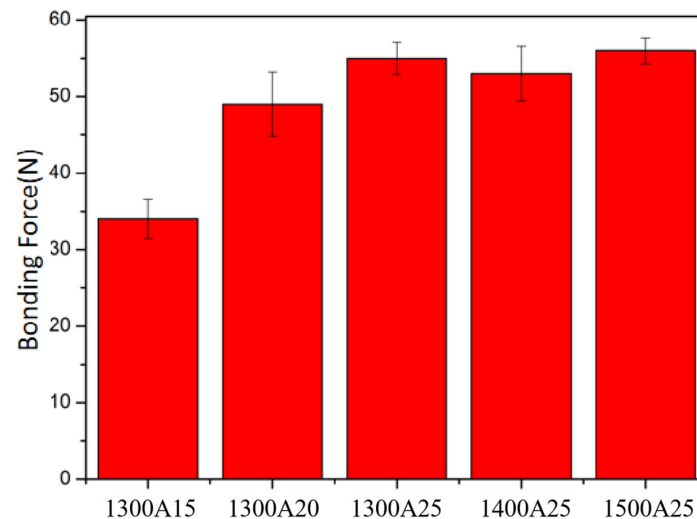
Figure 6. Bonding force of zirconia coating changes with sintering temperature and sintering time.

Then, phase analysis was performed on the coating samples sintered at different temperatures and times, and the test results are shown in Figure 7. The four curves from the bottom to the top are the XRD patterns of the zirconia coatings prepared when the sintering holding time is 10, 15, 20, and 25 min, respectively. It can be seen that the coatings exist in the form of tetragonal ZrO_2 sintered at 1300–1500 °C and different sintering times. Compared to Figure 5, it can be found that when the sintering temperature is higher than 1300 °C, ZrO_2 is a tetragonal calcium oxide and there is no existence of monoclinic zirconia. In addition, a small amount of C and Zr elements come from molds and reduction reactions at high temperatures.
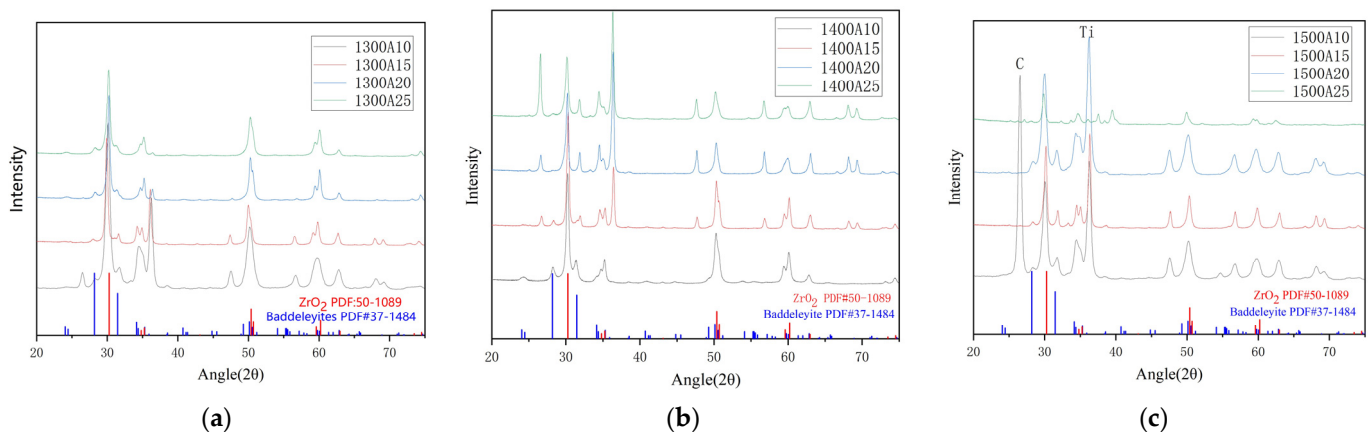

Figure 7. XRD patterns of zirconia coatings sintered at different temperatures: (**a**) 1300 °C, (**b**) 1400 °C, and (**c**) 1500 °C, and different sintering times.

Figure 8 shows the effect of the sintering temperature and sintering time on the hardness of the zirconia coatings. It can be seen that at a sintering temperature of 1300 °C, the hardness of the coating increases with the prolongation of the sintering time. However, at higher sintering temperatures (1400–1500 °C), the hardness of the coating first increases and then decreases with the increase in sintering time. This may be related to the process of grain sintering. In the initial stage, the increase in contact points between grains leads to an increase in the connection area, and prolonging the sintering time is beneficial for the increasing the density and compactness of the coating. As the sintering time increases, the neck of the grain connection expands, and the density and mechanical properties of coatings will be further improved. However, when the sintering time is too long, the growth of the grain size is too large, leading to a decrease in the number of grain boundaries [21].

Grain boundaries have an inhibitory effect on crack propagation, and excessive grain size can lead to uneven mechanical properties, ultimately resulting in a decrease in hardness. Generally, under the same sintering time, the hardness of the coating increases with the increase in sintering temperature. From the analysis of hardness values, the sintering time for obtaining the highest hardness will have a forward trend with the increase in sintering temperature. This further demonstrates the importance of an appropriate sintering time for improving the coating performance.
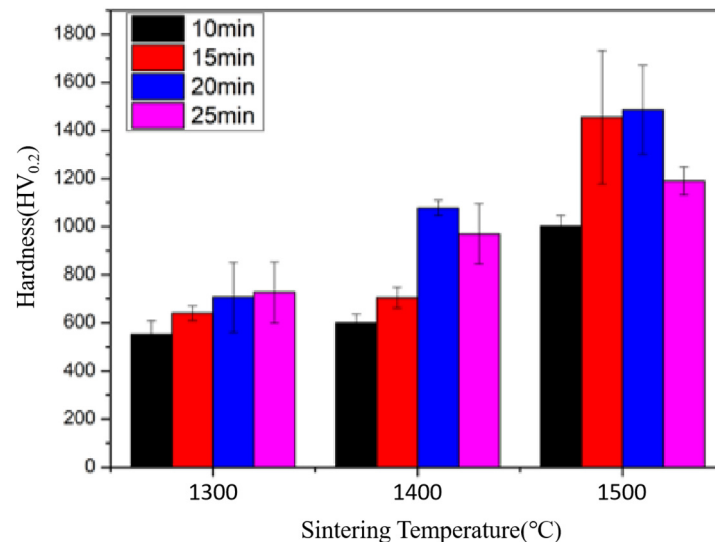

Figure 8. Hardness of zirconia coatings prepared at different sintering temperatures and sintering times.

3.2. The Influence of Coating Preparation Process Parameters on Tribological Performance

Si_3N_4 balls were selected as friction pairs to investigate the changes in the friction coefficient and wear rate of the titanium alloy substrate and coating surfaces under different loads. From Figure 9, it can be seen that, with the extension of running time, the friction coefficient of titanium alloy shows a slow upward trend, increasing from 0.3 to around 0.6. The friction coefficient decreases with the increase in load, and the wear rate of TC4 remains basically unchanged under different loads, which is about 9×10^{-7} $cm^3 \cdot N^{-1} \cdot m^{-1}$.
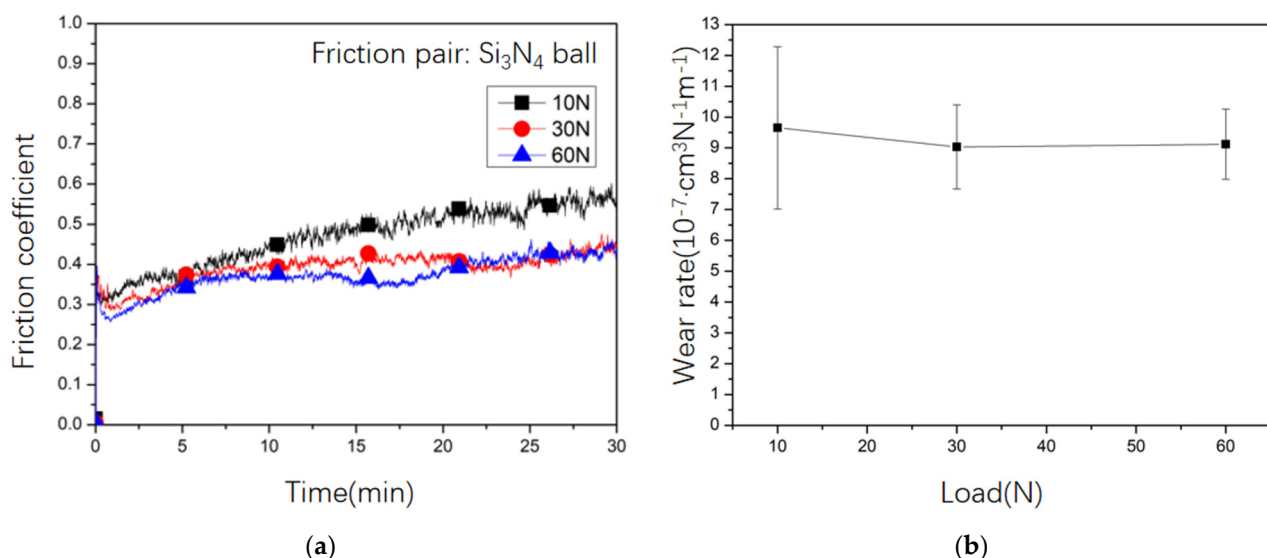

(**a**) (**b**)

Figure 9. Changes in the friction coefficient (**a**) and wear rate (**b**) of titanium alloy substrate under different loads.

Figure 10 shows the variation curve of the friction coefficient of zirconia coatings prepared under different sintering temperatures and sintering times. From Figure 10a, it can be seen that, under a low load, the friction coefficient of the coating is the lowest at a sintering time of 20 min when the sintering temperature is fixed. As shown in Figure 10b, it can be observed that when the sintering time is fixed at 20 min, the friction coefficient of the coating prepared at 1500 °C can be as low as about 0.3. Furthermore, with the increase in the load, the friction coefficient of coating shows a similar trend.
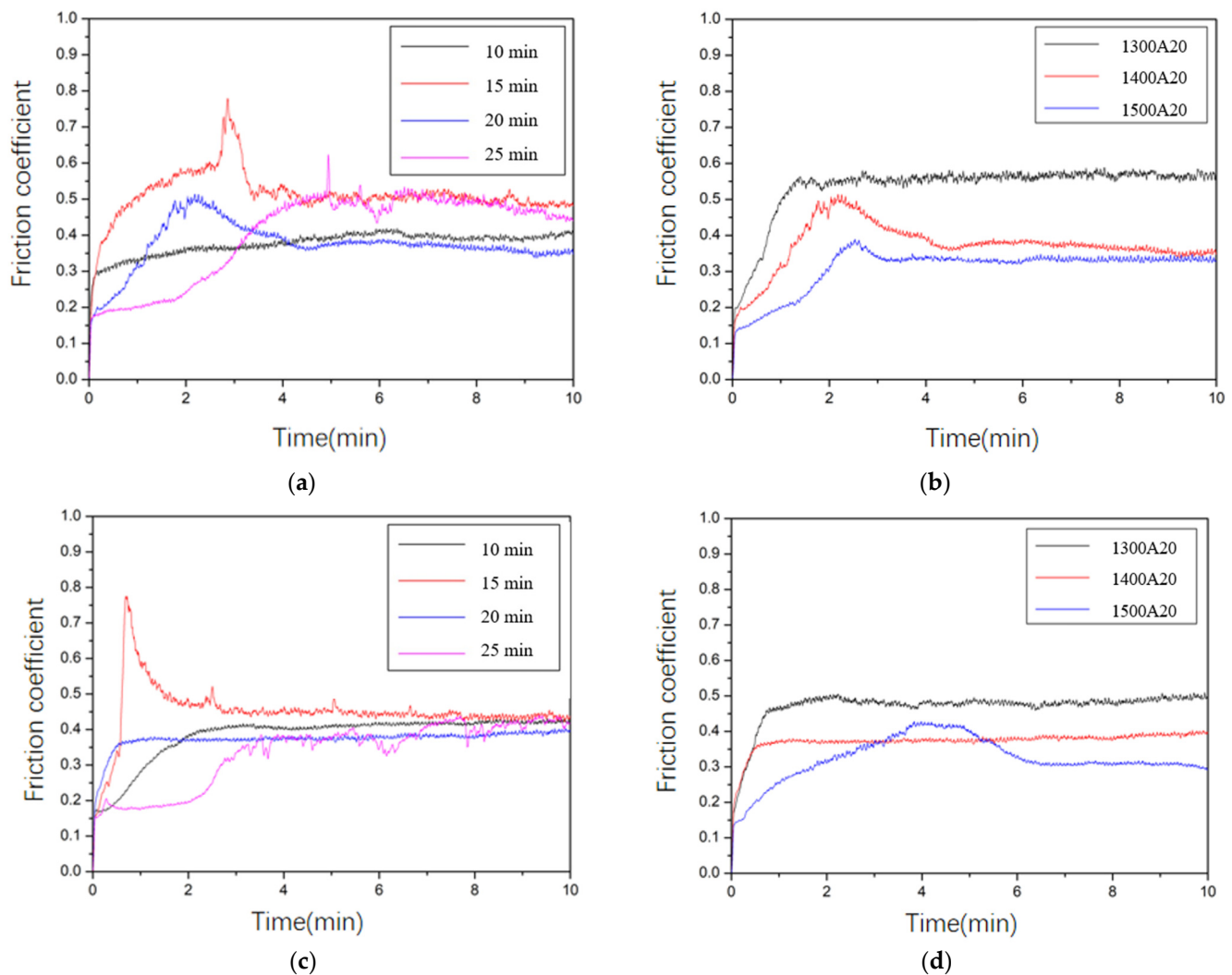

Figure 10. Friction coefficient variation curves of zirconia coatings prepared at 1400 °C with different sintering times (**a**,**c**) and at different sintering temperatures for 20 min (**b**,**d**) under different loads: 10 N (**a**,**b**) and 30 N (**c**,**d**).

Through the analysis of the friction coefficient results, it can be seen that the coating prepared under high-temperature sintering conditions has good anti-friction properties compared to titanium alloy substrates. The effect of the sintering time on the friction coefficient of the coating shows a trend of first decreasing and then increasing. This indicates that appropriate sintering parameters are beneficial in reducing the friction coefficient and improving the frictional properties of the coating. If the sintering temperature is too low and the sintering time is too short, the adhesion of the coating will be weak, and easy to peel off during the friction process. Excessive sintering time can lead to the formation of microcracks and the reduction in grain boundaries due to excessive grain size. Insufficient grain boundaries cannot hinder the formation of microcracks and can also easily generate debris, affecting the mechanical properties of the coating.

The wear rate is significantly affected by the sintering temperature and time. From Figure 11, it can be seen that, with the increase in the sintering temperature, the wear rate of coating shows a decreasing trend. This can be attributed to the high density, bonding strength, and hardness of the coating at higher sintering temperatures. The effect of sintering time on wear rate also shows a similar trend. In addition, the results indicate that the effect of the sintering temperature on the wear rate of zirconia coatings is more sensitive than the sintering time. It can be found that the 1500A20 zirconia coating shows the lowest wear rate, which is about 6.2×10^{-8} cm$^3 \cdot$N$^{-1} \cdot$m^{-1}. Compared to the titanium alloy substrate, the wear rate of sintered zirconia coating on its surface can be reduced by up to 93.1%.
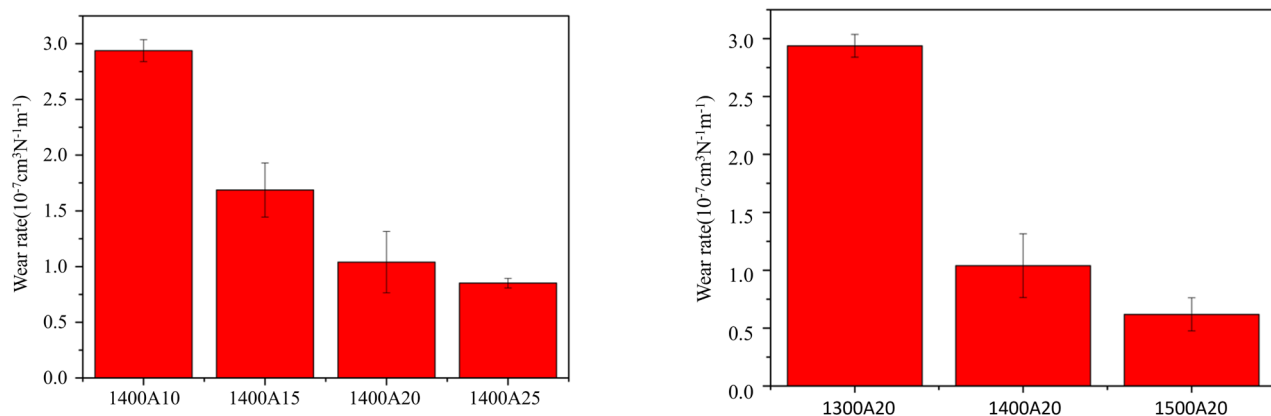

Figure 11. Variations in the wear rate of zirconia coatings prepared at different sintering times and sintering temperatures with the load of 30 N.

3.3. Analysis of Wear Mechanism

The interface diffusion behavior between the zirconia coating and TC4 titanium alloy is an important factor affecting the coating performance. Figure 12 illustrates the diffusion distance and concentration changes of the interface with increasing sintering time. The calculation process of diffusion is based on Fick's law (Formula (2)), where the diffusion coefficient can be expressed by the Arrhenius equation (Formula (3)), which makes the speed of diffusion directly related to temperature. The concentration–distance relationship of diffusion can be obtained through EDS line scanning, and the relevant parameters can be obtained to solve the diffusion equation after changing the sintering process conditions.

$$\frac{\partial c}{\partial t} = D \times \frac{\partial^2 c}{\partial x^2} \tag{2}$$

$$D = D_0 \times e^{\frac{-E}{RT}} \tag{3}$$

The diffusion distance between zirconia and Ti is influenced by the properties of the material itself, and the different diffusion coefficients lead to different diffusion distances. Therefore, zirconia has a longer diffusion distance. With the increase in sintering time, the diffusion distance at the interface between the coating and substances increases, which verifies the phenomenon detected in the experiment that the bonding force at the interface increases with the increase in sintering time.
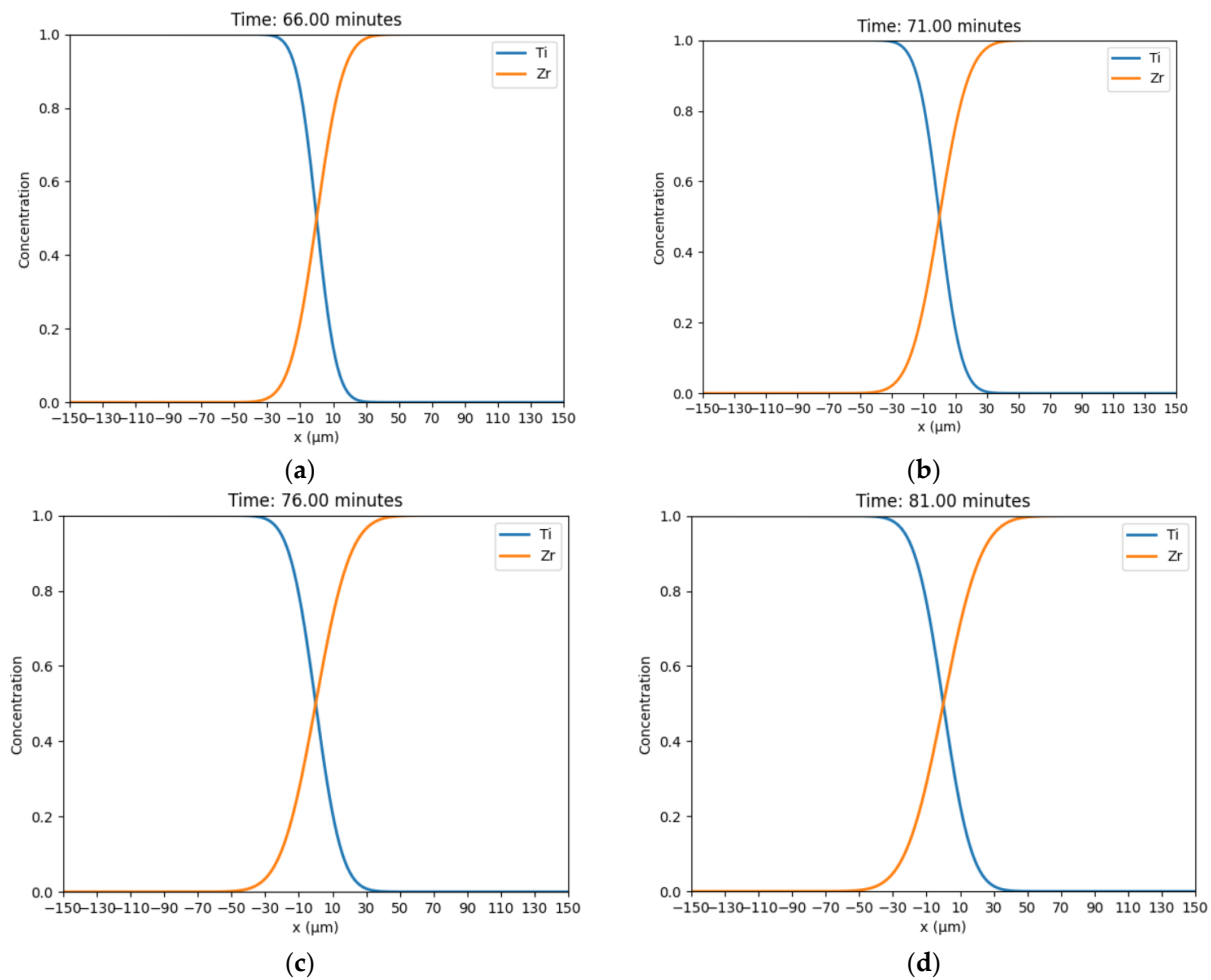
Figure 12. Fick's Law simulated interfacial diffusion process: sintering temperature at 1300 °C for different sintering times: (**a**) 10 min, (**b**) 15 min, (**c**) 20 min, (**d**) 25 min.

Figure 13 illustrates the influence of sintering temperature on the diffusion distance and concentration of zirconia at the interface. With the increase in sintering temperature, the diffusion distance of the Ti element has already exceeded 50 μm. Under this condition, the bonding force of the interface cannot be effectively detected by the scratch tester, resulting in a measurable ultimate bonding force of about 54 N.

Figure 14 shows a comparison of the wear morphologies of zirconia coatings prepared at different sintering temperatures. It can be seen that, under the same sintering time of 20 min, the coating prepared at a lower sintering temperature shows deeper wear tracks and obvious plow grooves on the surface after reciprocating friction (Figure 14(a1)). According to the SEM morphology, it can be observed that some areas of the wear tracks show the signs of coating peeling, or repeated rolling and sliding of the debris. Under high magnification, residual debris and crack marks on the surface can be obviously observed (Figure 14(a3)). This is mainly due to the lower density and hardness of the low-temperature sintered coating. As the sintering temperature increases, the surface of the coating prepared at 1400 °C shows a certain degree of layered wear, and the degree of plastic deformation of the coating also decreases (Figure 14(b3)). When the sintering temperature was further increased, the coating surface shows slight plowing grooves and a small amount of debris is generated on the surface (Figure 14(c3)). Under this condition, the high hardness and bonding strength of the coating play a major role.
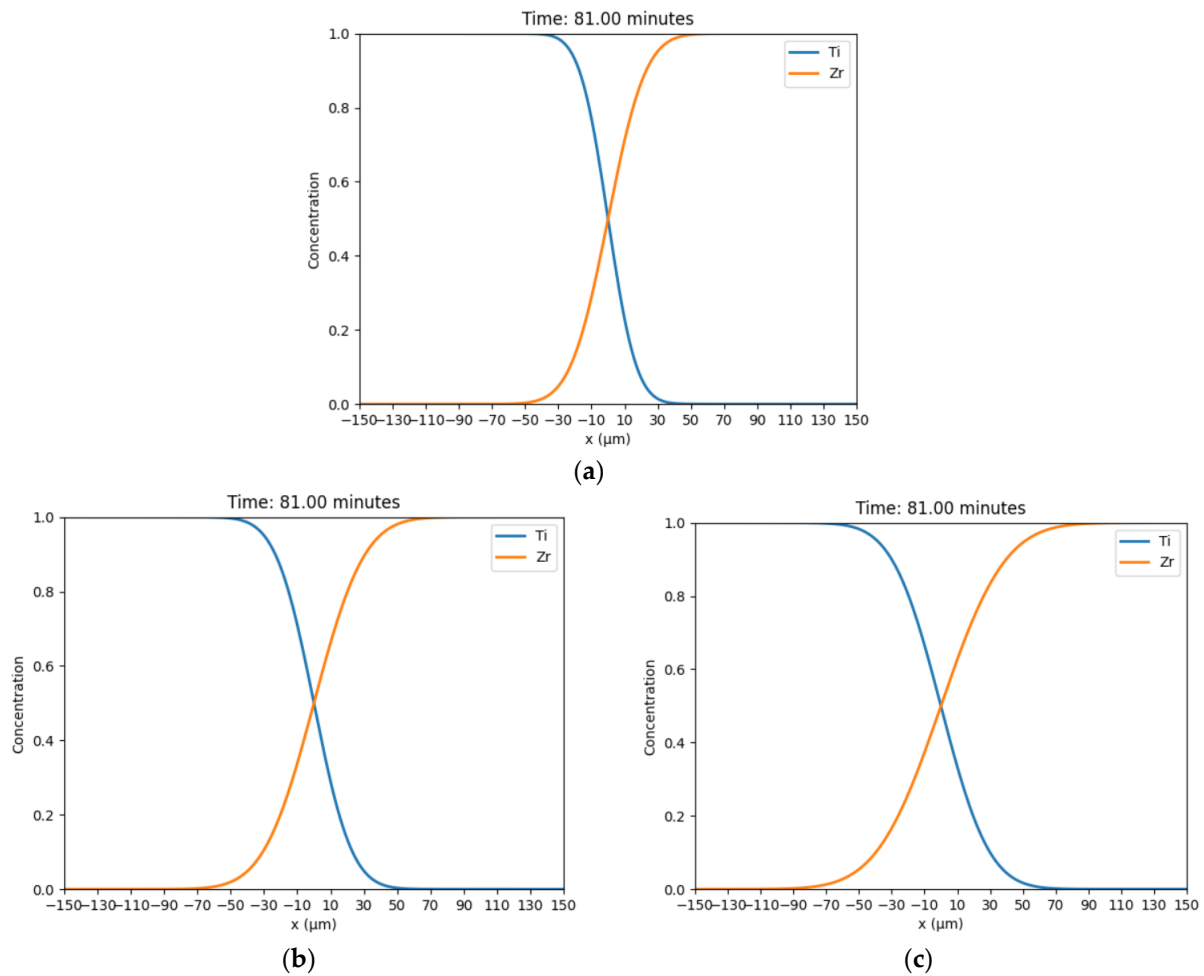
(**a**)

(**b**)

(**c**)

Figure 13. Fick's Law simulation interface diffusion process: sintering time at 25 min for different sintering temperatures: (**a**) 1300 °C, (**b**) 1400 °C, (**c**) 1500 °C.

Then, the worn surface morphologies of coatings prepared at different sintering times under a sintering temperature of 1400 °C were characterized, and the results are shown in Figure 13. It can be seen that when the sintering temperature is constant, the sintering time has a significant impact on the wear resistance of the coating. When the sintering time is 10 min and 15 min, the width of the worn track is much larger than that of the other coatings, resulting in obvious plow grooves and debris (Figure 15(a2,b2)). With the prolongation of sintering time, the wear volume of the coating decreases, and the wear of the coating becomes mild. The worn tracks of coatings are relatively smooth with only shallow scratches, especially for the 1400A25 coating (Figure 15(d3)). It can be considered that a longer sintering time reduces the surface pores and increases the hardness of coating while also improving the mechanical properties of materials such as adhesion force.

The Hertz contact models of Si_3N_4 balls in contact with the TC4 titanium alloy and zirconia coating were analyzed, and the results are shown in Figure 16. The Hertz pressure distribution and Hertz displacement are expressed in formulas as follows:

$$p = p_0(1 - \frac{r^2}{a^2})^{1/2} \tag{4}$$

$$u_z = (2a^2 - r^2), \ r \leq a \tag{5}$$

Among them, p_0 is the central stress, E^* is the equivalent elastic modulus, r is the horizontal distance from the center, and a is the radius of the contact area [22]. (TC4 has an elastic modulus of 110 GPa, Poisson's ratio of 0.34, silicon nitride has an elastic modulus of

320 GPa, Poisson's ratio of 0.26, zirconia has an elastic modulus of 210 GPa, and Poisson's ratio of 0.27).

The results indicate that, when the Si_3N_4 balls come into contact with TC4, the radius and depth of the contact area are higher than those of the zirconia coating, while the stress is slightly lower than that of the zirconia coating. The blue area in the figure represents the non-contact area which is subjected to a compressive stress of 0, but it does not mean that it is not under stress. Due to compression in the central area, the material sinks, and the area outside the Hertz contact area is subjected to tension from the material in the compressed area, resulting in a tensile stress. And, with the increase in r (horizontal distance from the center point in Formula (2)), the longitudinal displacement and tensile stress gradually decreases and eventually approaches 0. The mechanical properties of zirconia are affected by the sintering parameters. The 1500A20 zirconia coating with the highest hardness corresponding has the smallest Hertz contact area. Therefore, the zirconia coating shows less debris, and the lowest wear rate and wear volume.
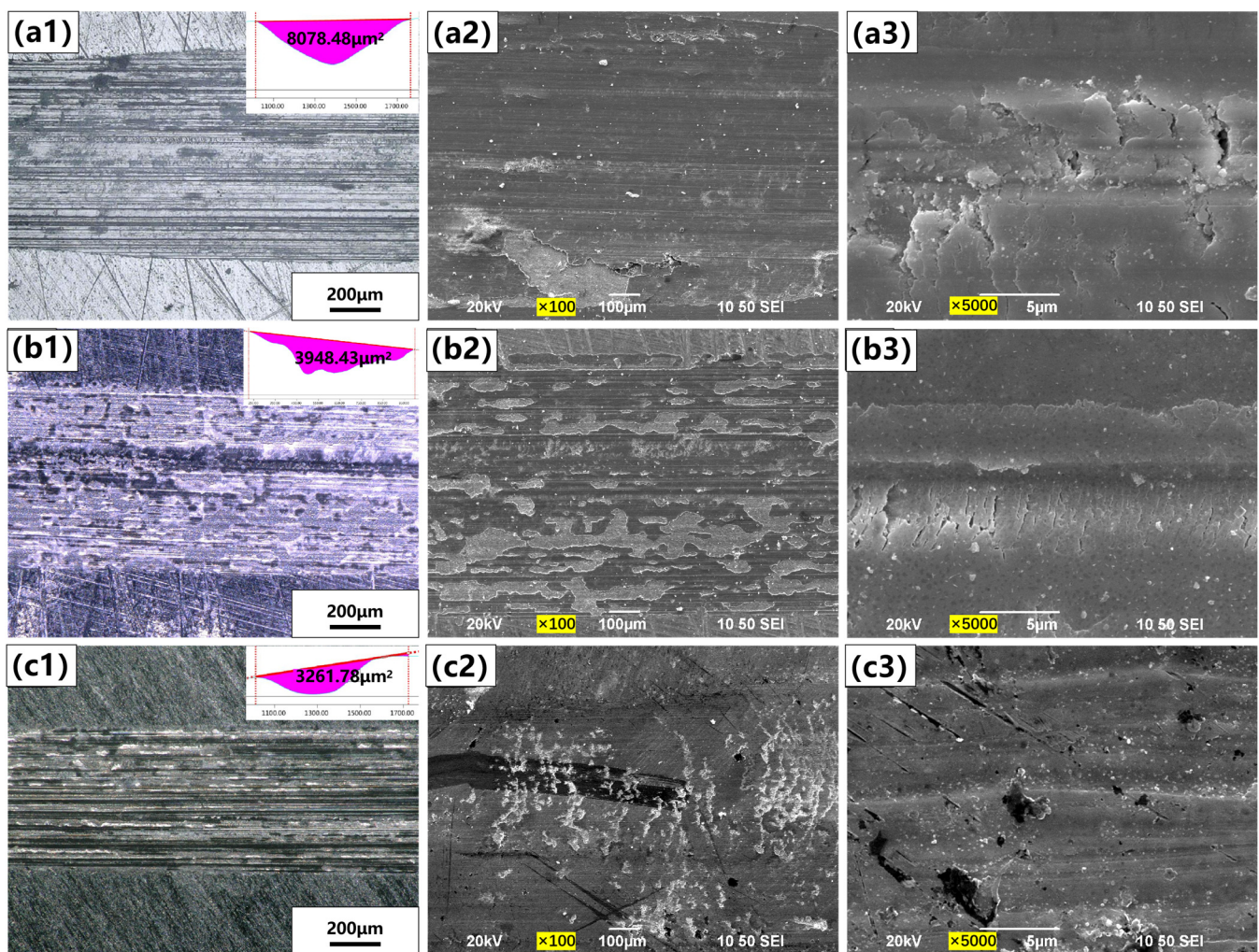

Figure 14. Optical micrographs of wear scars on zirconia coatings prepared at different sintering temperatures (**a1**) 1300 °C, (**b1**) 1400 °C, (**c1**) 1500 °C, and SEM micrographs of the worn surfaces at low magnification (**a2**–**c2**) and high magnification (**a3**–**c3**) (load of 30 N, sintering time of 20 min).
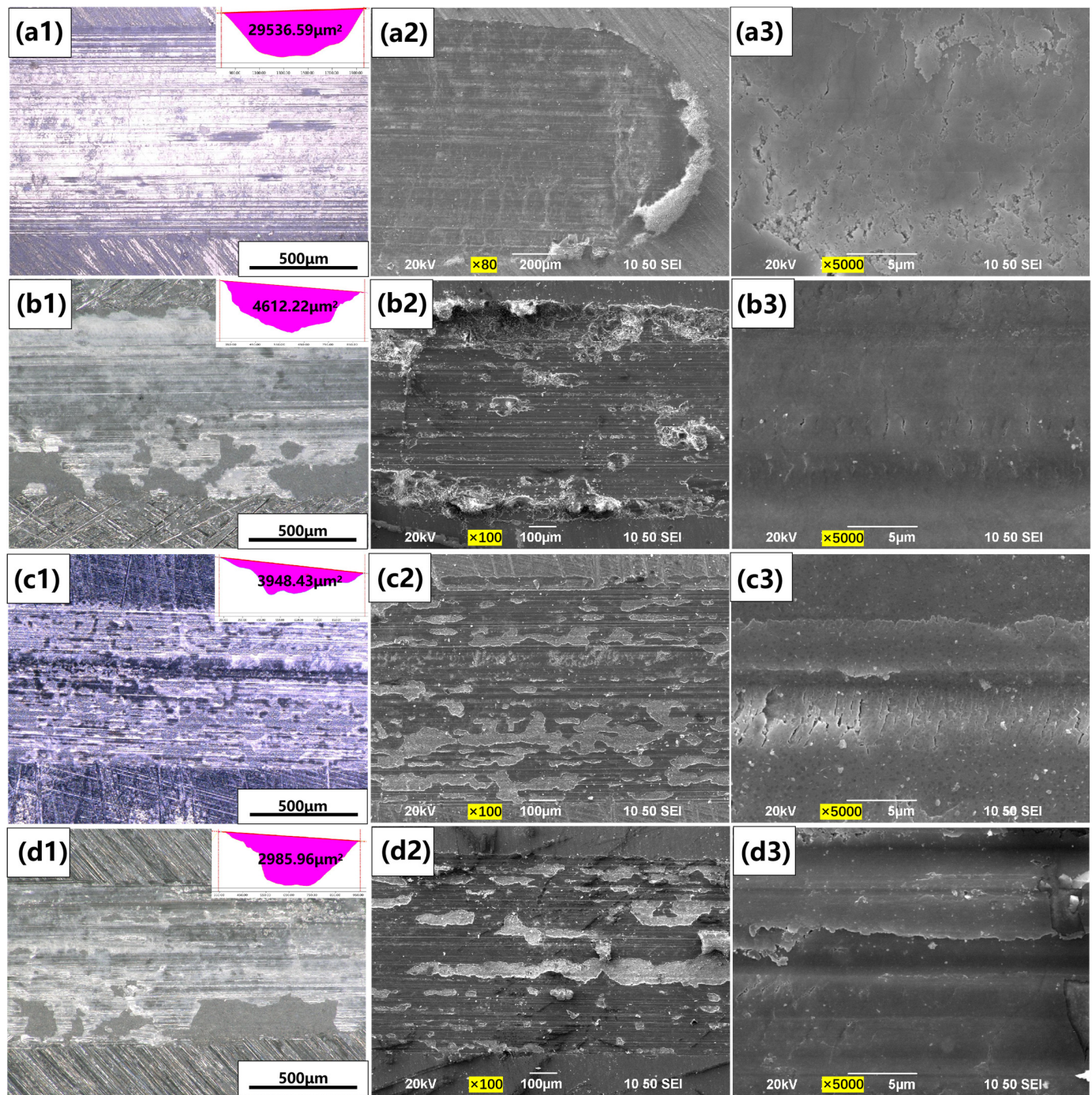
Figure 15. Optical micrographs of wear scars on zirconia coatings prepared at 1400 °C with different sintering times (**a1**) 10 min, (**b1**) 15 min, (**c1**) 20 min, (**d1**) 25 min, and the corresponding SEM micrographs at low magnification (**a2**–**d2**) and high magnification (**a3**–**d3**). Load of 30 N.
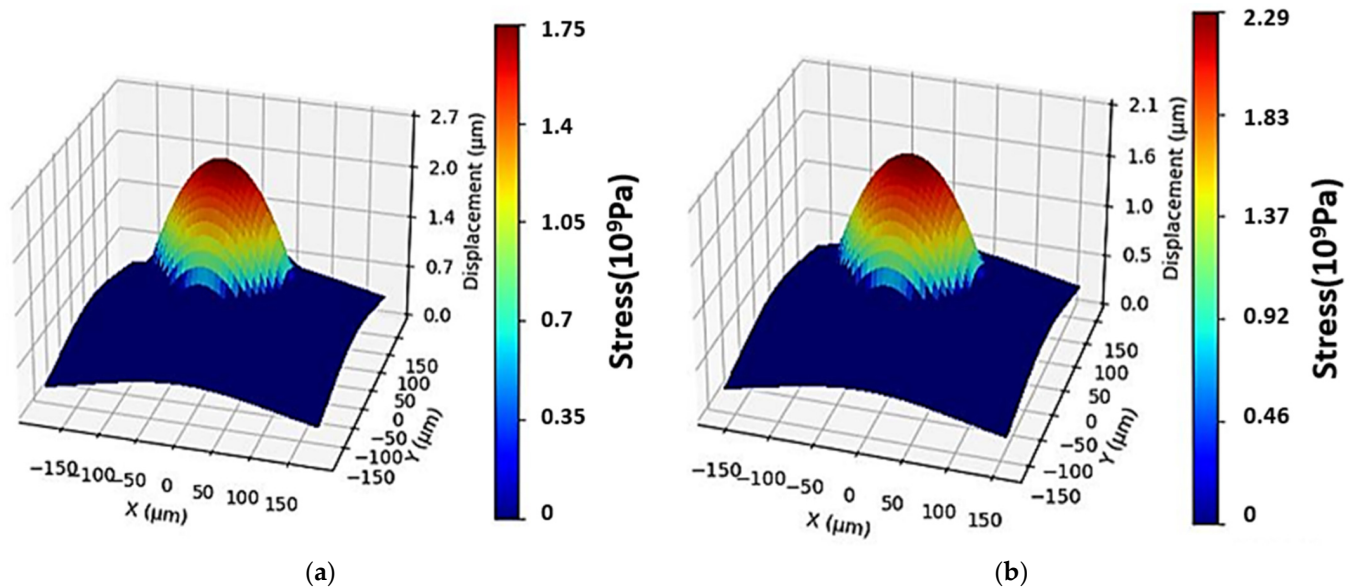
Figure 16. Hertz contact displacement maps of Si$_3$N$_4$ ball against TC4 (**a**) and ZrO$_2$ (**b**) under a load of 30 N. The colors represent the Hertz contact stress experienced.

4. Conclusions

Zirconia coatings were prepared on the surface of the titanium alloy using SPS. The influence of the sintering parameters on the mechanical and tribological properties of coatings was investigated. The experimental results were analyzed through numerical simulation and corresponding diffusion models, and wear mechanisms were proposed. The following conclusions have been drawn:

With the increase in sintering temperature, the density, bonding strength, and hardness of the zirconia coating are significantly improved. At sintering temperatures above 1400 °C, the density, bonding strength, and hardness of the coating show an overall trend of first increasing and then decreasing with the increase in sintering time. The coating has better mechanical properties when the sintering time is about 20 min.

At the appropriate sintering temperature and time, the frictional properties of the coating were optimized. Experimental results shows that the zirconia coating prepared at a sintering temperature of 1500 °C and a sintering time of 20 min has the lowest friction coefficient and wear rate, which are 0.33 and 6.2×10^{-8} cm^3·N^{-1}·m^{-1}, respectively. Compared to titanium alloy substrates, they can be reduced by 15.4% and 93.1%, respectively.

Fick's law was used to simulate the diffusion of zirconia and titanium during the sintering process. Increasing the sintering temperature and time helps to extend the diffusion distance, thereby enhancing the interfacial adhesion. The influence mechanism of different sintering temperatures and sintering times on the wear performance of zirconia coatings was explained using Hertz contact theory. The 1500A20 coating has the highest hardness, indirectly reflecting its higher elastic modulus. The contact area between the coating and Si$_3$N$_4$ ball is the smallest, indicating the optimal friction characteristics.

Author Contributions: Q.Z.: Writing—review and editing, supervision, resources, writing—original draft. T.H.: Writing—supervision, original draft, investigation, conceptualization, data curation. J.S.: Writing—review and editing, supervision, resources, funding acquisition, conceptualization, data curation. L.W.: Conceptualization, formal analysis. Y.S. and L.H.: Supervision. All authors have read and agreed to the published version of the manuscript.

Data Availability Statement: The original contributions presented in the study are included in the article, further inquiries can be directed to the corresponding author.

References

1. Chen, T.; Suryanarayana, C.; Yang, C. Advanced titanium materials processed from titanium hydride powder. *Powder Technol.* **2023**, *423*, 118504. [CrossRef]
2. Philip, J.T.; Mathew, J.; Kuriachen, B. Tribology of Ti6Al4V: A review. *Friction* **2019**, *7*, 497–536. [CrossRef]
3. Bansal, D.G.; Eryilmaz, O.L.; Blau, P.J. Surface engineering to improve the durability and lubricity of Ti–6Al–4V alloy. *Wear* **2011**, *271*, 2006–2015. [CrossRef]
4. Li, G.; Ma, F.; Liu, P.; Qi, S.; Li, W.; Zhang, K.; Chen, X. Review of micro-arc oxidation of titanium alloys: Mechanism, properties and applications. *J. Alloys Compd.* **2023**, *948*, 169773. [CrossRef]
5. Seth, S.; Jones, A.H.; Lewis, O.D. Wear resistance performance of thermally sprayed Al3Ti alloy measured by three body micro-scale abrasive wear test. *Wear* **2013**, *302*, 972–980. [CrossRef]
6. Weng, F.; Yu, H.; Chen, C.; Dai, J. Microstructures and wear properties of laser cladding Co-based composite coatings on Ti–6Al–4V. *Mater. Des.* **2015**, *80*, 174–181. [CrossRef]
7. Martini, C.; Ceschini, L. A comparative study of the tribological behaviour of PVD coatings on the Ti-6Al-4V alloy. *Tribol. Int.* **2011**, *44*, 297–308. [CrossRef]
8. Liu, J.; Xiong, J.; Guo, Z.; Qin, C.; Xiao, Y.; You, Q. Growth and Properties of $TiN/Al_2O_3/Ti(C, N)/TiN$ Multilayer CVD Coatings on Ti (C, N)-Based Cermet Substrates with Ni, Co and Fe Binders. *Metall. Mater. Trans. A* **2019**, *51*, 863–873. [CrossRef]
9. She, D.; Liu, S.; Kang, J.; Yue, W.; Zhu, L.; Wang, C.; Wang, H.; Ma, G.; Zhong, L. Abrasive Wear Resistance of Plasma-Nitrided Ti Enhanced by Ultrasonic Surface Rolling Processing Pre-Treatment. *Materials* **2019**, *12*, 3260. [CrossRef]
10. Guo, J.; Wang, F.; Liou, J.J.; Liu, Y. Preparation and Tribological Properties of a Superhydrophobic TB6 Titanium Alloy. *Mater. Res.-Ibero-Am. J. Mater.* **2023**, *26*, e20220446. [CrossRef]
11. Tang, C.B.; Liu, D.X.; Zhang, Q.; Zhang, X.H. Effect of Ti/Mo and Cr/Mo metallic multilayer films on fretting fatigue resistance of Ti-6Al-4V alloy. *Mater. Res. Innov.* **2011**, *15*, 166–170. [CrossRef]
12. Mohammed, M.T.; Hussein, S.M. Synthesis and characterization of nanocoatings derived by sol–gel onto a new surgical titanium surface. *Mater. Res. Express* **2019**, *6*, 076426. [CrossRef]
13. Cai, X.; Gao, Y.; Cai, F.; Zhang, L.; Zhang, S. Effects of multi-layer structure on microstructure, wear and erosion performance of the Cr/CrN films on Ti alloy substrate. *Appl. Surf. Sci.* **2019**, *483*, 661–669. [CrossRef]
14. Zhang, L.C.; Chen, L.Y.; Wang, L. Surface Modification of Titanium and Titanium Alloys: Technologies, Developments, and Future Interests. *Adv. Eng. Mater.* **2020**, *22*, 1438–1656. [CrossRef]
15. Dejun, K.; Jing, Z.; Hao, L. Friction-wear behaviours of micro-arc oxidation films in situ grown on 7475 aluminium alloys. *Mater. Technol.* **2017**, *32*, 737–743. [CrossRef]
16. Katsui, H.; Shimoda, K.; Hotta, M. Preparation of silicon carbide and tantalum carbonitride composite with high hardness and moderate elastic modulus by laser chemical vapor deposition for anti-erosion protective coatings. *Ceram. Int.* **2023**, *49*, 38813–38823. [CrossRef]
17. Beresnev, V.M.; Smolyakova, M.Y.; Pogrebnyak, A.D.; Kaverina, A.S.; Drobyshevskaya, A.A.; Svetlichnyy, E.A.; Kolesnikov, D.A. Studying tribological characteristics of alumina- and zirconia-based ceramics. *J. Frict. Wear* **2014**, *35*, 137–140. [CrossRef]
18. Rylski, A.; Siczek, K. The Effect of Addition of Nanoparticles, Especially ZrO_2-Based, on Tribological Behavior of Lubricants. *Lubricants* **2020**, *8*, 23. [CrossRef]
19. Balaji, V.S.; Surendarnath, S. High-Temperature Wear Behavior of Spark-Plasma Sintered Titanium/(TiB + TiC) In Situ Composites. *Trans. Indian Inst. Met.* **2019**, *72*, 1669–1673. [CrossRef]
20. Zhao, X.; Duan, L.; Wang, Y. Fast interdiffusion and Kirkendall effects of SiC-coated C/SiC composites joined by a Ti-Nb-Ti inter layer via spark plasma sintering. *J. Eur. Ceram. Soc.* **2019**, *39*, 1757–1765. [CrossRef]
21. Zhao, J.; Gao, K.; Liu, D.; Ma, T.; Sun, D.; Gao, Y.; Pan, K.; An, L. Sintering Process in hot oscillatory pressure of 90W-7Ni-3Fe refractory alloy at different time. *Vacuum* **2022**, *195*, 110697. [CrossRef]
22. Popov, L.V. Chapter 5 The exact solution of contact problem—Hertzian contact. In *Contact Mechanics and Friction Physical Principles and Applications*, 2nd ed.; Li, Q., Luo, J., Eds.; Tsinghua University Press: Beijing, China, 2019; Volume 5, pp. 77–84.